Quantifying the impact of genetic determinants of antibiotic resistance on bacterial lineage dynamics

David Helekal[1], Tatum D. Mortimer[2], Aditi Mukherjee[1], Samantha G. Palace[1], Yonatan H. Grad[1]

[1] Department of Immunology and Infectious Diseases, Harvard T. H. Chan School of Public Health, Boston, Massachusetts, USA

[2] Department of Population Health, College of Veterinary Medicine, University of Georgia, Athens, Georgia, USA

Running title: Fitness impact of resistance determinants

Keywords: pathogen phylodynamics; antimicrobial resistance; *Neisseria gonorrhoeae*; adaptation; fitness

ABSTRACT

The dynamics of antimicrobial resistance in bacteria are informed by the fitness advantages conferred by genetic determinants of resistance in the presence of antibiotic pressure and the potential fitness costs in its absence. However, frameworks for quantitative estimates of real-world fitness impact have been lacking, given multidrug resistance, multiple pathways to resistance, and uncertainty around drug exposures. Here, we addressed these challenges through analysis of genome sequences from clinical isolates of *Neisseria gonorrhoeae* collected over 20 years from across the United States, together with national data on antibiotic treatment. Using a hierarchical Bayesian phylodynamic model, we quantified the contributions of resistance determinants to strain success. Resistance mutations had a fitness benefit when the cognate antibiotic was in use but did not always incur a fitness cost otherwise. Two fluoroquinolone-resistance conferring mutations at the same site in *gyrA* had divergent fitness impact after fluoroquinolones were no longer used for treatment, findings supported by *in vitro* competition experiments. Fitness costs were alleviated by loss of costly resistance determinants and counterbalanced by gain of new fitness-conferring resistance determinants. Quantifying the extent to which the resistance determinants explained each lineage's dynamics highlighted gaps and pointed to opportunities for investigation into other genetic and environmental drivers. This work thus establishes a method for linking pathogen genomics and antibiotic use patterns to quantify the fitness impact of resistance determinants and the factors shaping ecological trends.

INTRODUCTION

The prevalence of antimicrobial resistance (AMR) reflects competition in an ever-changing environment [1, 2]. When an antibiotic is introduced into clinical use, it can result in increased fitness and prevalence of resistant bacteria. Once resistance to the antibiotic becomes sufficiently widespread, its use is often reduced in favor of another antibiotic for which resistance prevalence is low. This alters the fitness landscape, such that alleles and genes that had conferred a fitness advantage in the context of the first antibiotic may become deleterious.

The complexity of the bacterial AMR fitness landscape is shaped by multiple factors. These include antibiotic pressure from drugs in current and past use as well as antibiotic resistance, which can often be achieved through multiple, at times interacting, genetic pathways (c.f., macrolide resistance in *N. gonorrhoeae* [3] and fluoroquinolone resistance in *E. coli* [1]). Population structure [4, 5], linkage between AMR determinants in a changing environment [1, 5], linkage with sites under balancing selection [6, 5], mutation-selection balance [7], and non-antibiotic pressures can all also inform this landscape.

While the genetic determinants of AMR play a large role in the population expansion and contraction of drug resistant lineages [1], the fitness impact of these determinants can vary across genetic backgrounds and environment [8, 9]. Efforts to quantify the fitness impact of individual genetic features across shifting patterns of antibiotic use in real world data have been fraught with many challenges, such as limited availability of data on antimicrobial use, both for targeted treatment and accounting for bystander exposure [10]; the influence of other factors, such as pressure from host immunity, on overall pathogen fitness; and the frequent co-occurrence of multiple antibiotic resistance determinants in drug resistant strains [4, 5]. Additionally, for many pathogens, we lack longitudinal datasets of sufficient size, duration, and systematic collection to enable inference about fitness.

Here, we overcame these challenges to define the fitness contributions of AMR determinants in response to changes in treatment using data from *N. gonorrhoeae* in the USA. *N. gonorrhoeae* is an obligate human pathogen that causes the sexually transmitted infection gonorrhea; infection does not elicit a protective immune response [11, 12]. A collection of over 5000 specimens from 20 years (2000-2019) of the CDC's Gonococcal Isolate Surveillance Project (GISP), the CDC's sentinel surveillance program for

antibiotic resistant gonorrhea, have been sequenced and have undergone resistance phenotyping, with metadata including the demographics of the infected individuals [3, 13, 14, 15, 16]. Data on primary treatment in the US over this period have been reported by the CDC and reflect changes in first-line therapy, from fluoroquinolones to cephalosporins plus macrolides, and, among the cephalosporins, from the oral cefixime to intramuscular ceftriaxone [17]. Together, these factors enabled us to estimate quantitatively the resistance determinant-specific fitness costs in circulating *N. gonorrhoeae* and their interaction with antibiotic pressures.

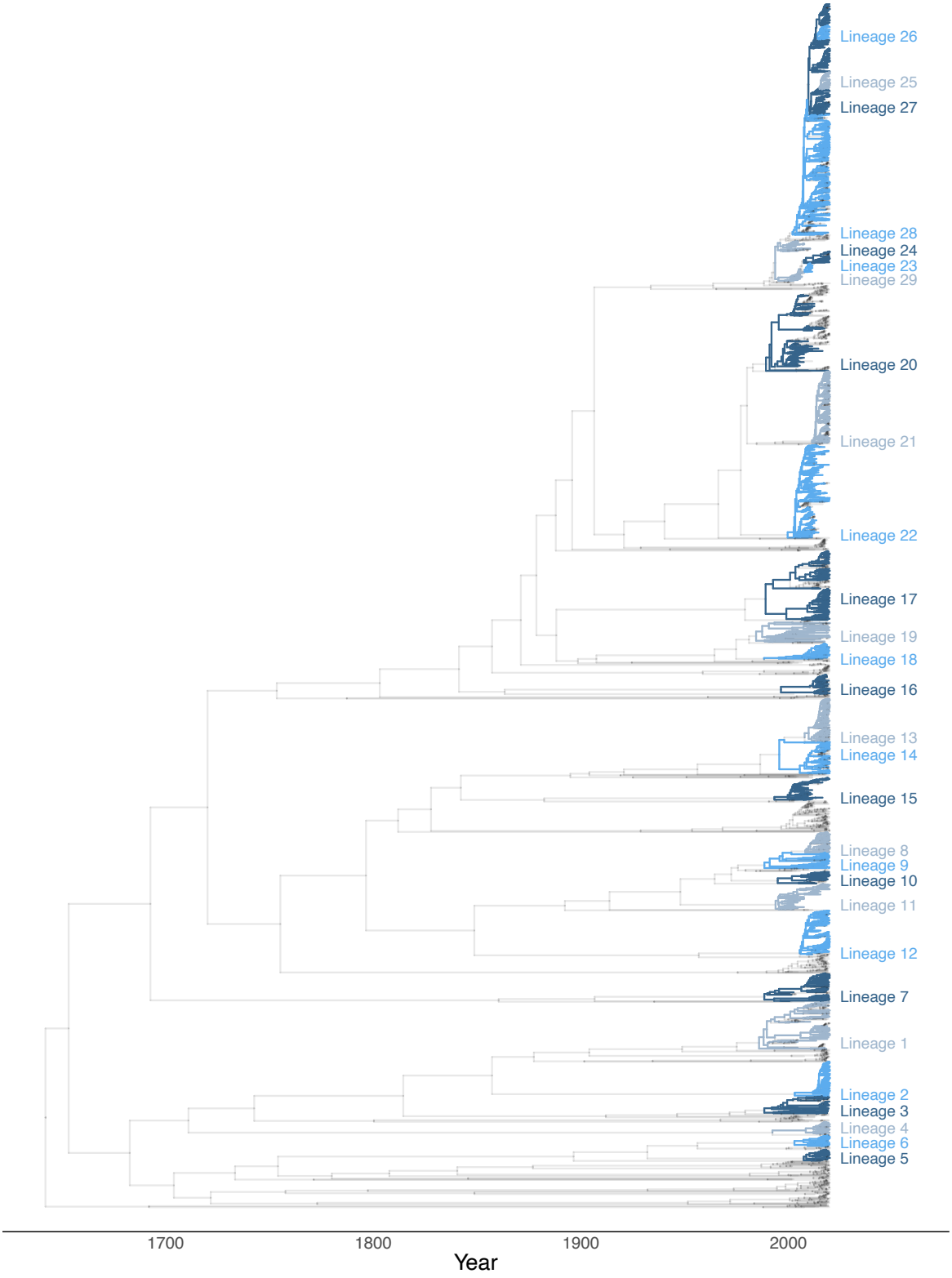

Figure 1: Lineage assignment based on AMR determinants. The phylogenetic tree is annotated according to the lineage assignment of the ancestral node. Gray nodes in the phylogenetic tree denote lines of descent that are not in an assigned lineage. Lineage numbering was determined by post-order traversal of the tree.

	gyrA		*parC*			*ponA*	*penA*			*mtr*				*23S rRNA*
Lineage	S91	D95	D86	S87	E91	L421	A501	G543	Type	*mtrC*	*mtrD*	*mtr* promoter	*mtrR*	C2611
1	S	D	D	S	E	L	A	G	non-m	non-m	non-m	non-m	LOF	C
2	S	D	D	S	E	L	A	G	non-m	non-m	non-m	non-m	non-m	C
3	S	D	D	S	E	L	A	G	non-m	non-m	non-m	non-m	non-m	C
4	S	D	D	S	E	L	A	G	non-m	non-m	non-m	non-m	non-m	C
5	S	D	D	S	E	L	A	G	non-m	non-m	non-m	non-m	non-m	C
6	S	D	D	S	E	L	A	G	non-m	non-m	non-m	non-m	non-m	C
7	S	D	D	S	E	P	A	G	non-m	non-m	non-m	A-del	non-m	C
8	S	D	D	S	E	L	A	G	non-m	non-m	non-m	non-m	non-m	C
9	S	D	D	S	E	P	A	G	non-m	non-m	non-m	non-m	non-m	C
10	S	D	D	S	E	P	A	G	non-m	non-m	non-m	A-del	non-m	C
11	S	D	D	S	E	P	A	G	non-m	non-m	non-m	A-del	non-m	C
12	F	G	D	S	G	P	T	G	non-m	non-m	non-m	A-del	non-m	C
13	F	A	D	R	E	L	A	G	non-m	non-m	non-m	non-m	LOF	C
14	F	A	N	S	E	L	A	G	non-m	non-m	non-m	non-m	LOF	C
15	F	G	D	R	E	P	A	G	non-m	non-m	non-m	A-del	non-m	C
16	F	G	N	S	E	P	V	G	non-m	non-m	non-m	A-del	non-m	C
17	S	D	D	S	E	P	A	G	non-m	non-m	non-m	A-del	non-m	C
18	S	D	D	S	E	L	A	G	non-m	non-m	non-m	non-m	non-m	C
19	S	D	D	S	E	P	A	G	non-m	non-m	non-m	non-m	non-m	C
20	F	G	D	R	E	P	A	S	non-m	non-m	non-m	A-del	non-m	C
21	F	A	D	R	E	P	A	S	non-m	non-m	non-m	non-m	non-m	C
22	F	G	D	R	E	P	—	—	mosaic	non-m	non-m	A-del	non-m	C
23	S	D	D	S	E	L	—	—	mosaic	non-m	non-m	non-m	non-m	C
24	S	D	D	S	E	L	A	G	non-m	non-m	non-m	non-m	non-m	C
25	S	D	D	S	E	L	A	G	non-m	non-m	mosaic	mosaic	non-m	C
26	F	A	N	S	E	L	A	G	non-m	mosaic	mosaic	mosaic	non-m	C
27	S	D	D	S	E	L	A	G	non-m	mosaic	mosaic	mosaic	non-m	C
28	S	D	D	S	E	L	A	G	non-m	non-m	mosaic	non-m	non-m	C
29	S	D	D	S	E	L	A	G	non-m	non-m	non-m	non-m	non-m	T

Table 1: Distribution of AMR determinants across lineages in (Figure 1). Gray color corresponds to wild type allele. For *gyrA*, *parC* and *ponA*, polymorphisms occur at several key amino acid positions. The *penA* and *mtr* loci exhibit complex patterns of polymorphism that include interspecies mosaicism as well as individual amino acid variations. `non-m` denotes non-mosaic alleles. `Adel` denotes `A` deletion in the *mtrR* promoter [18]. `LOF`=loss of function. The only determinant in 23S rRNA that appears frequently in our dataset is the C2611T substitution, where `T` indicates at least one and up to four copies of 23S rRNA C2611T. Coloring highlights non-wild type determinants in each column and changes from column to column.

RESULTS

Defining *N. gonorrhoeae* Drug Resistant Lineages

We first sought to define AMR-linked lineages from the GISP specimens. On epidemic timescales [20], *N. gonorrhoeae* maintains a lineage structure largely shaped by antimicrobials [21]. The treatment for *N. gonorrhoeae* infections in the US over the past 20 years has been defined by three main drug classes: fluoroquinolones, third generation cephalosporins, and macrolides (Supplementary Figures and Tables Figure S1). We used ancestral state reconstruction for the major AMR determinants for these antibiotics to identify clusters of specimens that had not changed state since descending from their most recent common ancestors (MRCA). We refined the classification by requiring that the MRCA was no earlier than 1980. As the three drug classes under study entered use after this date, this

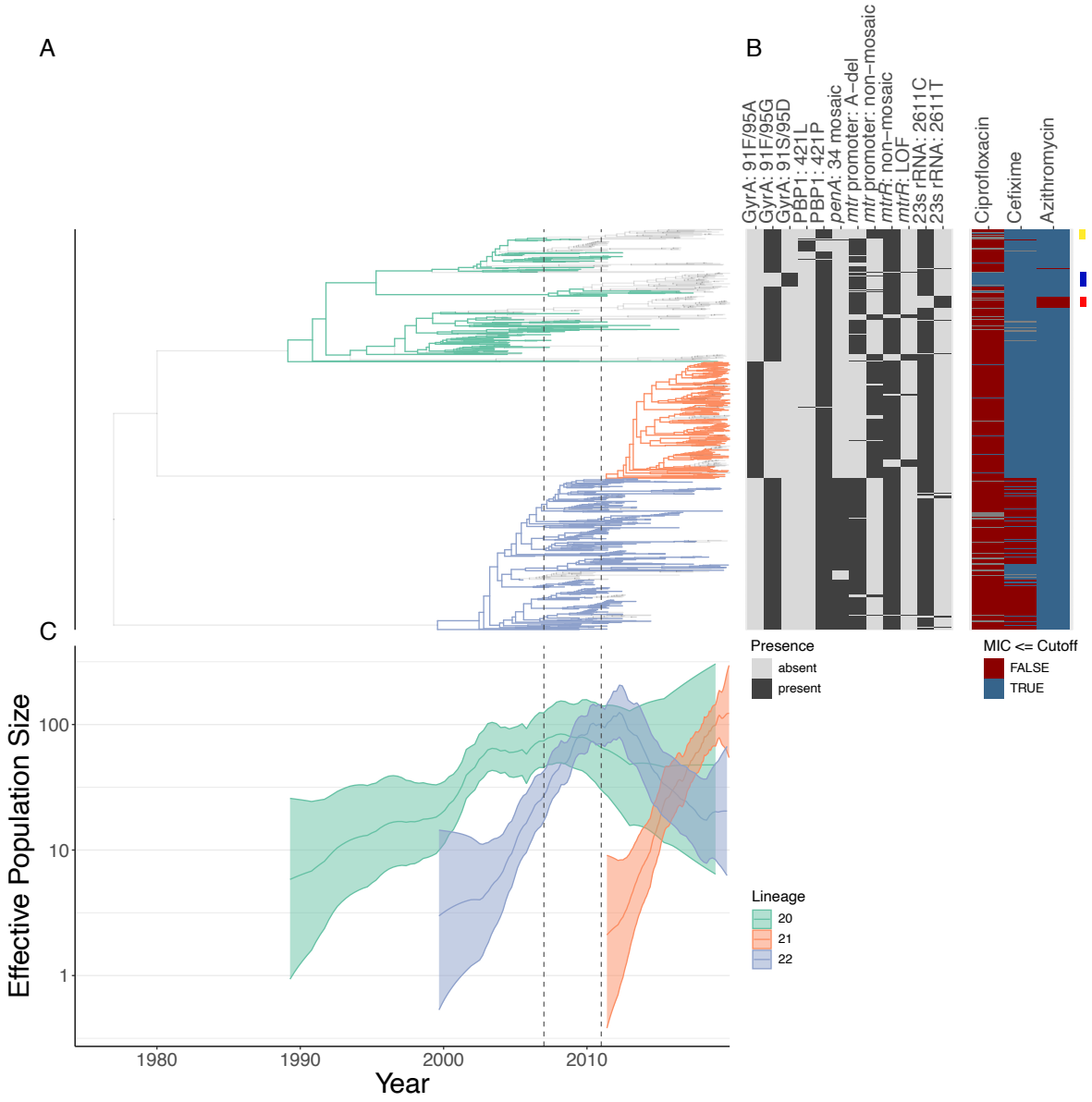

Figure 2: A cluster of phylogenetically related lineages shows evidence of adaptation in response to changes in antibiotic use. Panel A: the phylogeny for lineages 20-22. The gray transparent tips correspond to isolates that have diverged from the ancestral motif combination of the parental lineage. Panel B: the presence and absence of relevant resistance mutations and antibiotic resistance phenotypes above or below each drug's cutoff (CIP: 1µg/mL; CFX: 0.25µg/mL, AZI: 4µg/mL). The yellow bar on the right highlights a cluster of isolates that changed *mtr* promoter alleles. The blue bar on the right highlights a cluster of isolates that reverted to a fluoroquinolone-susceptible *gyrA* allele. Red bar on the right highlights a cluster of isolates that acquired azithromycin resistance. Panel C: Median effective population size trajectories for each of the lineages with 95% credible intervals as estimated by `phylodyn` [19].

cutoff limits the analysis to a time frame over which ancestral state reconstruction is likely to remain accurate, while helping separate lineages that acquired the same resistance pattern independently. We focused on lineages that have at least 30 specimens, reasoning that a minimum cutoff helps avoid the inclusion of small outbreak clusters that could potentially produce unreliable estimates (see Methods Lineage Assignment & Phylogenetic Reconstruction).

This definition led to the identification of 29 lineages across the dataset (Figure 1), along with the corresponding distribution of determinants (Table 1). The majority of lineages (21/29) have at least one AMR determinant, with multiple pathways to resistance for a given antibiotic present across lineages. Lineages 22 and 23, for example, carry the mosaic *penA* 34 allele, and the remaining 27 lineages all carry the Penicillin Binding Protein 2 (PBP2; encoded by *penA*) substitution $A517G$, each of which increases resistance to cephalosporins [22, 23].

The related lineages $20 - 22$ share many resistance determinants but have differing estimates of their effective population sizes through time, $Ne(t)$, and illustrate the dynamics that emerge when juxtaposing $Ne(t)$ with antibiotic use and resistance (Figure 2). This cluster of lineages contains a previously described and the largest mosaic *penA* 34-carrying lineage, lineage 22 [3], along with its two sister-lineages. Lineage 20, the oldest lineage in this cluster, grew during the fluoroquinolone era and decreased afterwards [24]. In this lineage, nearly all descendants sampled after the recommendation of ceftriaxone plus azithromycin dual therapy had acquired a new resistance determinant or lost an existing one. In one sublineage, this change included replacement of a resistance-conferring *gyrA* allele (encoding 91F, 95G) with the wild-type allele (91S, 95D), resulting in phenotypic susceptibility (Figure 2, blue bar). Another sublineage changed *mtrR* promoter alleles (Figure 2, yellow bar). Determinants at the *mtrR* promoter are associated with resistance to a wide range of antibiotics [18] including macrolides [25]. Yet another sublineage acquired azithromycin resistance through C2611T substitution in 23S rRNA (Figure 2, red bar). Furthermore, the descendants of Lineage 20 appeared to switch sexual networks: most recent isolates were from heterosexuals whereas past isolates were from men who have sex with men (Supplementary Figures and Tables Figure S2). Lineage 21 expanded after the 2010 switch in recommended treatment to dual therapy with azithromycin plus ceftriaxone. The effective population size for the mosaic *penA* 34-carrying lineage 22 grew during the fluoroquinolone period and after, but decreased with the introduction of azithromycin and ceftriaxone dual therapy. Together, these patterns of lineage expansion and contraction indicated a relationship

among the antibiotics recommended for treatment, genetic determinants of resistance, and lineage success. However, while for lineages 20 and 22 the pattern of expansion an contraction aligns matches our expectations based on their resistance profile, it was not clear from a simple inspection what could explain the dynamics of lineage 21.

Hierarchical Bayesian Phylodynamic Modeling Reveals a Changing Fitness Landscape

We next sought to quantify the fitness contributions of the genetic determinants of resistance and how these varied over time. For each determinant, we estimated a set of regression coefficients, one for each of the antibiotic classes to which it conferred resistance, along with an intercept term. These modeled the effect of a given resistance determinant on the effective population size growth rate of lineages that carry that determinant as a function of the reported treatments (Supplementary Figures and Tables Table S1). As the treatment data are percentages summing to 1 and thus are not full rank, we selected ceftriaxone 250mg as the baseline for all estimated treatment use effects. (See Sections A Lineage-Based Hierarchical Phylodynamic Model and Supplementary Methods A Hierarchical Phylodynamic Model for explicit formulation of the model).

This model formulation allowed us to answer three main questions. First, did the relative fitness of a given resistance determinant change as a function of the pattern of antibiotic use? Second, what is the fitness cost or benefit through time associated with a particular resistance allele compared to its susceptible counterpart? Third, how much of a lineage's trajectory is explained by the fitness contributions of the resistance determinants? To answer these questions, we first calculated the predicted effect of individual determinants on the growth rate of lineages, finding that several resistance determinants had a strong impact (defined by the 95% posterior credible interval interval excluding $[-0.1, 0.1]$) on lineage dynamics (Supplementary Figures and Tables Table S2).

gyrA *gyrA* is the main fluoroquinolone-resistance determining gene in *N. gonorrhoeae*, with alleles of *parC* also contributing to resistance [25]. Our modeling revealed several phenomena among lineages encoding ParC 86D/87R/91E. First, lineages carrying GyrA 91F/95G with this *parC* allele experienced a growth rate increase during the period of recommended fluoroquinolone treatment for gonorrhea

(Figure 3, Supplementary Figures and Tables Figure S3). However, for GyrA 91F/95G, there was too much uncertainty to determine its absolute effect on the growth rate of lineages carrying it during the fluoroquinolone period compared to the baseline GyrA 91S/95D type within the wild-type ParC 86D/87S/91E context (Figure 3). After fluoroquinolones were no longer recommended, GyrA 91F/95G appeared weakly deleterious when combined with ParC 86D/87R/91E allele compared to wild type (Figure 3, Supplementary Figures and Tables Table S2). Second, lineages carrying GyrA 91F/95A had distinctly higher growth rates than the GyrA 91S/95D susceptible allele after the period in which fluoroquinolones were used for treatment (Figure 3, Supplementary Figures and Tables Table S2). Third, lineages carrying GyrA 91F/95A had a relative growth rate advantage over GyrA 91F/95G after the end of fluoroquinolone era (Supplementary Figures and Tables Figure S4). The majority of lineages carrying GyrA 91F/95A expanded after 2007, increasing the uncertainty in estimates of the effect that fluoroquinolone use had on these lineages.

To investigate whether the resistance provided by GyrA 91F/95G differed from GyrA 91F/95A in lineages containing the ParC 86D/87R/91E allele, we fitted a linear model to $\log_2$-transformed ciprofloxacin MIC, while accounting for determinants at the *mtrCDE* operon. There was no significant difference in $\log_2$-transformed ciprofloxacin MICs (GyrA 91F/95G coefficient = 0.183, two-sided T-test P-value > 0.242; see Supplementary Methods Comparison of the Impact of GyrA 91F/95G versus GyrA 91F/95A on ciprofloxacin MICs for details).

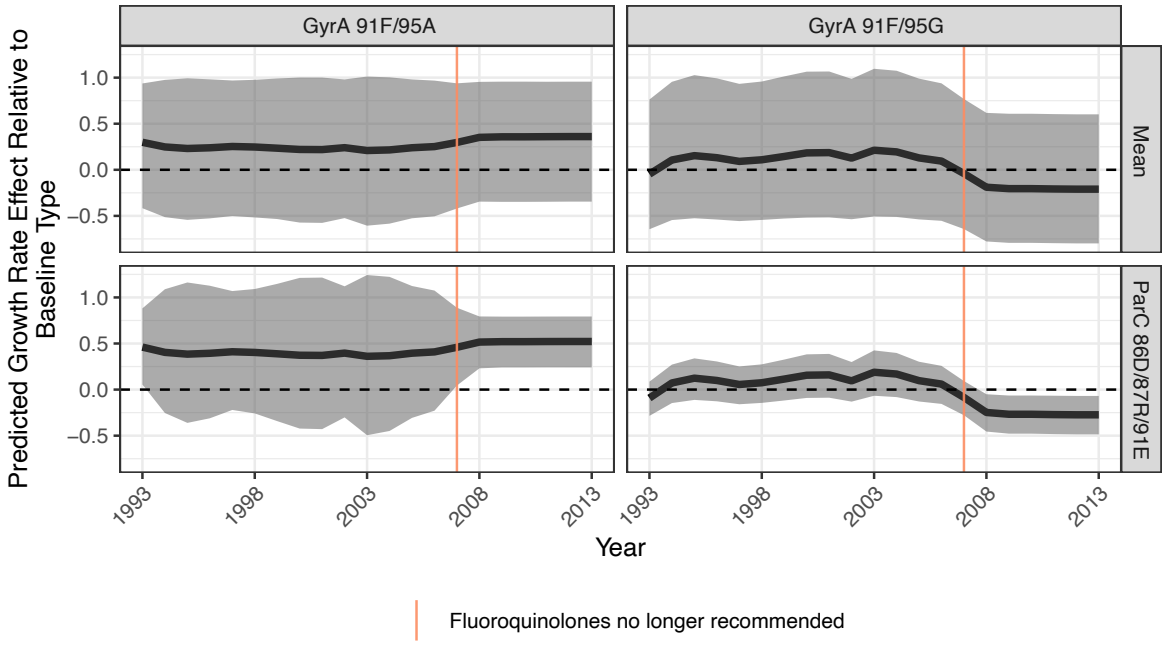

Figure 3: The estimated predicted effect on growth rate of selected GyrA motifs within the ParC 86D/87R/91E context based on past fluoroquinolone use patterns. The predicted effect is an absolute effect as computed compared to the baseline GyrA 91S/95D type within the wild-type ParC 86D/87S/91E context. The average effect across all *parC* contexts for each of the *gyrA* alleles is denoted by Mean. The shaded region denotes the 95% posterior credible interval around the posterior median, depicted by the bold black line. Dashed line denotes no predicted growth rate effect relative to baseline allele.

Given these results, we tested whether GyrA 91F/95A contributes to a growth rate advantage over GyrA 91F/95G *in vitro*. Both sets of mutations increased the ciprofloxacin MIC ≥128-fold over the susceptible *gyrA* allele (Supplementary Figures and Tables Table S3). In a competition assay between GyrA 91F/95A and GyrA 91F/95G isogenic strains in the GCGS0481 strain background with ParC 86D/87R/91E, GyrA 91F/95A conferred a fitness benefit (Figure 4): the competitive index (CI) after 8 hours of competition for GCGS0481 kanamycin-labeled GyrA 91F/95A versus GyrA 91F/95G was 1.54 ($p = 0.0003$), consistent with the reciprocal competition, in which the CI of kanamycin-labeled GyrA 95F/95G versus GyrA 91F/95A was 0.54 ($p = 0.0017$). Both GyrA 91F/95G and GyrA 91F/95A strains were less fit than the susceptible parental strain (Supplementary Figures and Tables Figure S5). After 8 hours of competition, the CI of kanamycin-labeled GyrA 91F/95A versus GyrA 91S/95D was 0.67 ($p = 0.0015$), and for kanamycin-labeled GyrA 91F/95G versus GyrA 91S/95D, it was 0.58 ($p = 0.0009$) (Supplementary Figures and Tables Figure S5). Consistent with this, the CI after 8

hours of competition of GCGS0481 kanamycin-labeled GyrA 91S/95D versus GyrA 91F/95A was 1.45 (p = 0.0023) and kanamycin-labeled GyrA 91S/95D versus GyrA 91F/95G was 1.72 (p = 0.0001) (Supplementary Figures and Tables Figure S5).

GyrA 91F/95A within the ParC 86N/87S/91E context conferred a growth rate advantage after 2007, when fluoroquinolones were no longer in use, compared to the baseline type that does not carry any of the resistance determinants studied (Supplementary Figures and Tables Table S2, Supplementary Figures and Tables Figure S6).

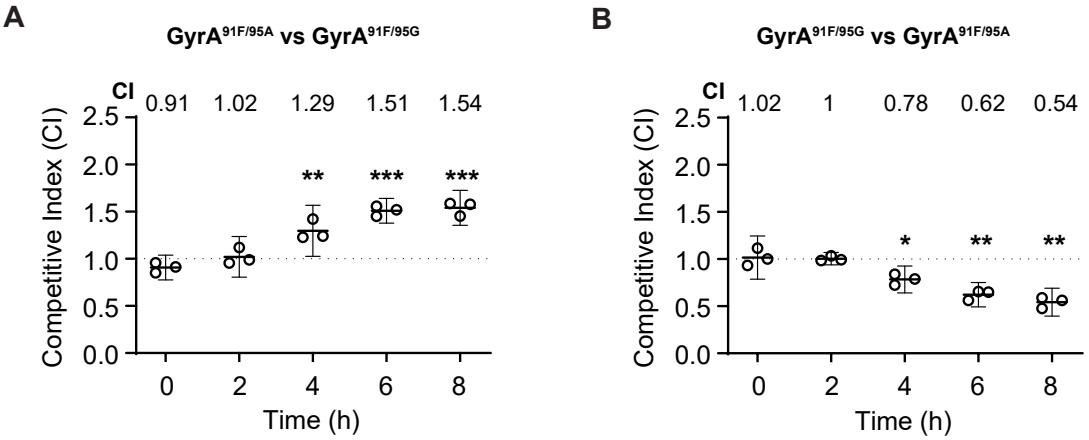

Figure 4: *In vitro* competition assays between GCGS0481 GyrA 91F/95A and GyrA 91F/95G with ParC 86D/87R/91E. Panel A: Competition between unlabeled GCGS0481 GyrA 91F/95G and kanamycin-labeled GyrA 91F/95A. Statistical significance (for 2, 4, 6 and 8 hours, p = 0.13, 0.005, 0.0002, 0.0003, respectively). Panel B: Competition between unlabeled GCGS0481 GyrA 91F/95A and kanamycin-labeled GyrA 91F/95G. Statistical significance (for 2, 4, 6 and 8 hours, p = 0.84, 0.02, 0.003, 0.0017, respectively). N = 3/time point, representative of three independent experiments performed in the absence of antibiotic pressure. Error bars represent mean with 95% CI. Statistically significant differences in CI values were analyzed using an unpaired two-sided Student's *t test* ($^*p < 0.05$, $^{**}p < 0.005$ and $^{***}p < 0.0005$).

penA The *penA* gene, which encodes PBP2, contributes to resistance to cephalosporins as well as other beta lactams, with mosaic *penA* alleles the major determinants of resistance to cephalosporins [26, 13, 27]. Most of the cephalosporin resistance determinants in our dataset appeared in 1-3 lineages each (Table 1), which limited our ability to estimate their impact on growth rates (Supplementary Figures and Tables Table S2, Figure S7). However, we estimated a major beneficial effect of mosaic *penA* 34 on growth rates when cefixime and ceftriaxone 125mg were widely used, as well as the subsequent loss of this beneficial effect when treatment with cephalosporins other than ceftriaxone

250mg declined. (Figure 5, Supplementary Figures and Tables Table S2). Similarly, carriage of PBP2 501T was associated with a large relative decrease in fitness when ceftriaxone 250mg became the sole recommended treatment (Supplementary Figures and Tables Table S2, Figure S7). However, the absolute effect for PBP2 501T compared to wild-type cannot be identified (Supplementary Figures and Tables Table S2, Figure S7), as PBP2 501T appeared only in a single lineage that carries a unique GyrA/ParC combination. The decrease in the predicted growth rate effect for both mosaic *penA* 34 and PBP2 501T started in 2008 and aligns with a shift in primary treatment with cephalosporins to ceftriaxone 250mg, even before the guidelines changed in 2012 (Supplementary Figures and Tables Figure S1).

PBP2 501V was associated with a weak increase in fitness after the switch in treatment to ceftriaxone 250mg (Supplementary Figures and Tables Table S2, Supplementary Figures and Tables Figure S8). Both the PBP2 501V and 501T have wide credible intervals for their absolute effects compared to the baseline type that does not carry any of the resistance determinants studied (Supplementary Figures and Tables Table S2, Supplementary Figures and Tables Figure S7). These alleles occur both in a single lineage each with a unique *gyrA*/*parC* combinations (Table 1) making the intercept term for these determinants unidentifiable.

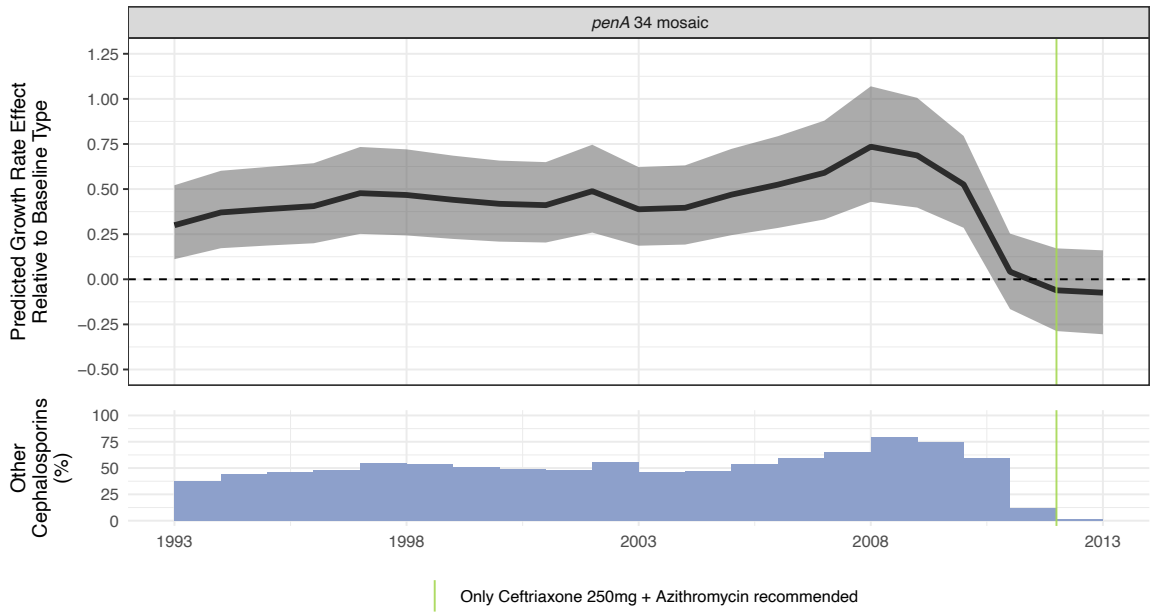

Figure 5: Top Panel: The predicted the absolute growth rate effect for mosaic *penA* 34 compared to baseline. The predicted effect was computed based on reported treatments. The shaded region denotes the 95% credible interval around the posterior median, depicted by the bold black line. Dashed line denotes no predicted growth rate effect relative to the baseline type that does not carry any of the resistance determinants studied. Bottom Panel: The use of cephalosporins other than ceftriaxone 250mg as a percentage of primary treatment. Other cephalosporins consist mainly of ceftriaxone 125mg, cefixime and other unclassified cephalosporins.

ponA The *ponA* gene encodes Penicillin Binding Protein 1 (PBP1) and contributes to resistance to penicillin [28]. The PBP1 421P variant was associated with a weak disadvantage compared to the baseline type that does not carry any of the resistance determinants throughout the study period. (Supplementary Figures and Tables Table S2, Figure S9, Figure S10).

***mtr* locus** *mtrCDE* encodes an efflux pump that modulates resistance to a wide range of antibiotics in *N. gonorrhoeae* [18], including to macrolides [25], and it is regulated by its transcriptional repressor, MtrR. Of particular relevance are mosaic *mtrC*, *mtrD*, and *mtrR* promoter as these are associated with azithromycin resistance [3, 29]. While our modeling recovered a growth rate increase associated with the carriage of mosaic *mtrR* promoter and the mosaic *mtrD* compared to wild-type baseline during the azithromycin co-treatment era (Supplementary Figures and Tables Table S2, Supplementary Figures and Tables Figure S11), the fact that mosaic *mtrR* promoter only occurred on mosaic *mtrD* backgrounds in our dataset (Table 1) raises the concern that the estimated effects of the *mtrR* promoter

and the mosaic *mtrD* maybe be only weakly identified. As such, we focused on the combined effect of mosaic *mtrR* promoter, mosaic *mtrC*, and mosaic *mtrD*. The predicted combined effect had large uncertainty, limiting interpretation, with clear support for a growth rate benefit only in 2010-2011 (Figure 6).

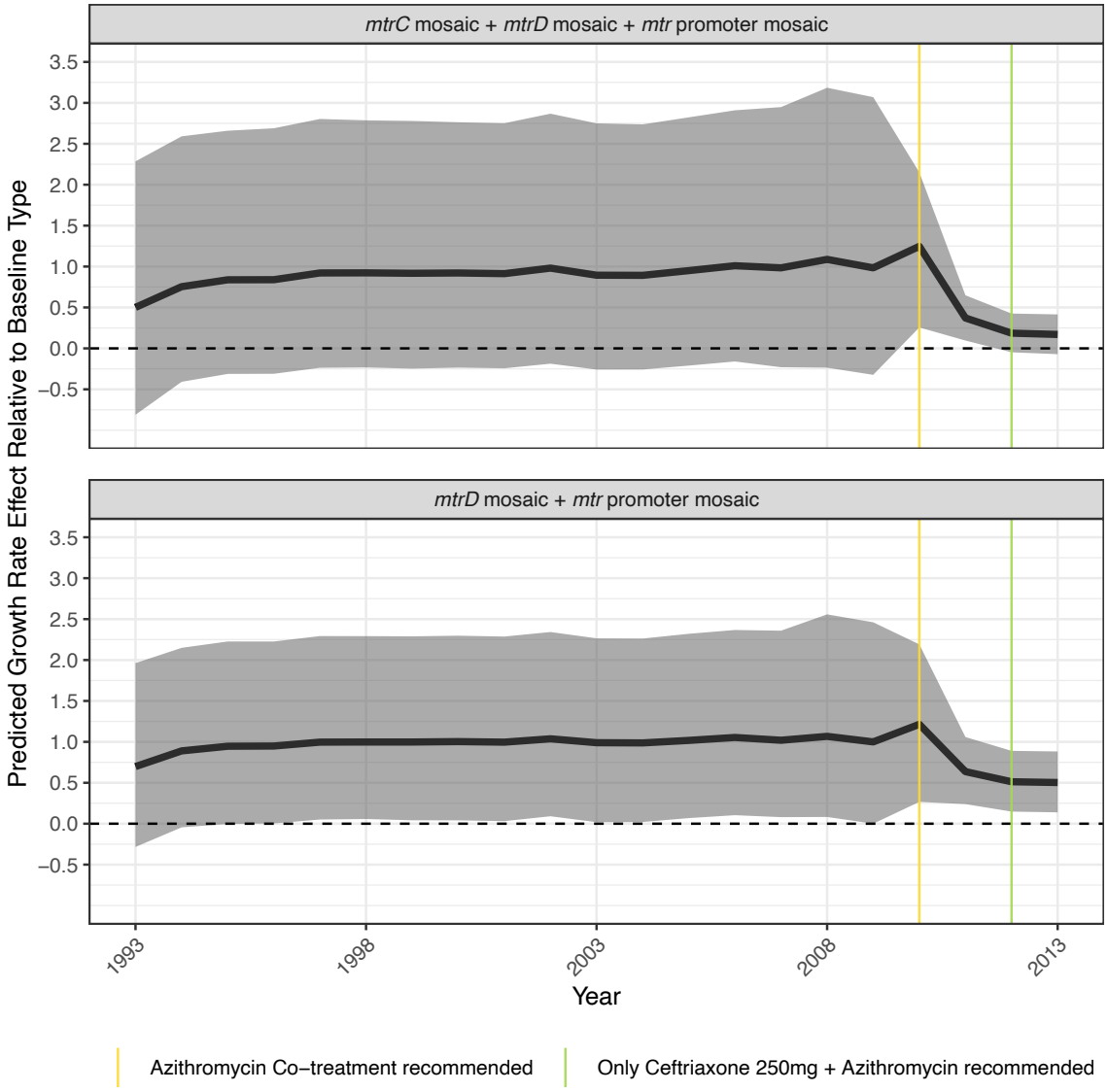

Figure 6: Predicted absolute effect for the total impact of the two most common combinations of determinants at the *mtrCDE* locus. The predicted effect was computed based on reported treatments. The shaded region denotes the 95% credible interval around the posterior median, depicted by the bold black line. Dashed line denotes no predicted growth rate effect relative to the baseline type that does not carry any of the resistance determinants studied.

The *mtrR* promoter A deletion in the 13-bp inverted repeat – a determinant implicated in an increase in resistance to a wide range of antibiotics including macrolides [18] – was associated with a weak increase in growth rate after the switch to ceftriaxone 250mg and azithromycin. This increase led to a weak advantage in growth rate after 2012 compared to the baseline type that does not carry any of the resistance determinants studied (Supplementary Figures and Tables Table S2, Supplementary Figures and Tables Figure S11, Supplementary Figures and Tables Figure S12).

Extent of lineage growth trajectory explained by resistance determinants

To quantify the extent to which the set of resistance determinants and lineage background explains each lineage's growth rate over time, for each lineage we visualized the average growth rate effect of individual resistance determinants, along with lineage residual effect and lineage background effect, and summarized the total effect in the four treatment recommendation periods in the study period (Figure 7, Supplementary Figures and Tables Figures S13 to S40).

This per-lineage analysis revealed the shifting contributions of resistance determinants to individual lineage growth dynamics, provided examples in which fitness costs of one determinant are counterbalanced by the fitness benefits of another, and identified lineages with dynamics unexplained by these determinants. Lineage 22 carried a combination of GyrA 91F/95G along with mosaic *penA* 34. Despite carrying GyrA 91F/95G, which was associated with a fitness cost after fluoroquinolones were no longer recommended in 2007 (Figure 3, Supplementary Figures and Tables Table S2), the growth of this lineage peaked in 2010, reflecting the fitness benefit of the mosaic *penA* 34 (Figure 7). The shift in use to cephalosporins plus azithromycin in 2010 was accompanied by a fitness benefit from *mtr* variants, though cumulatively the fitness costs from other resistance determinants resulted in an overall negative growth rate.

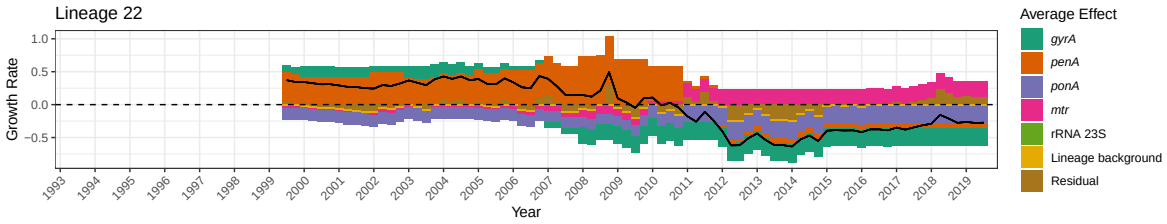

Contribution	1993–2007	2007–2010	2010–2012	2012–2019
gyrA	0.10 (−0.13, 0.30)	−0.20 (−0.40, −0.01)	−0.27 (−0.48, −0.07)	−0.27 (−0.48, −0.07)
penA	0.42 (0.21, 0.67)	0.67 (0.39, 0.98)	0.28 (0.10, 0.50)	−0.07 (−0.30, 0.16)
ponA	−0.19 (−0.39, −0.02)	−0.16 (−0.42, 0.08)	−0.20 (−0.38, −0.05)	−0.26 (−0.46, −0.05)
mtr	−0.01 (−0.21, 0.17)	−0.09 (−0.36, 0.17)	0.13 (−0.16, 0.42)	0.24 (0.03, 0.45)
rRNA 23S	–	–	–	–
Lineage background	−0.01 (−0.18, 0.12)	−0.01 (−0.18, 0.12)	−0.01 (−0.18, 0.12)	−0.01 (−0.18, 0.12)
Residual	−0.01 (−0.13, 0.12)	−0.02 (−0.27, 0.23)	0.00 (−0.26, 0.27)	−0.02 (−0.18, 0.13)
AMR Total	0.32 (0.05, 0.55)	0.22 (−0.12, 0.55)	−0.07 (−0.37, 0.25)	−0.37 (−0.62, −0.12)
Total	0.29 (0.06, 0.50)	0.18 (−0.09, 0.42)	−0.09 (−0.37, 0.19)	−0.41 (−0.56, −0.26)

Figure 7: Growth rate effect summary for Lineage 22. The top panel shows the combined average growth rate effect of resistance determinants along with the lineage background term and the residual. The black solid line represents the total average effect. The dashed horizontal line indicates zero. The bottom panel depicts a table summarizing the median total growth rate effect across 4 treatment periods, as well as the 95% credible interval around the median in brackets. The period 1993-2007 corresponds to when fluoroquinolones were recommended as primary treatment; 2007-2010 to when multiple cephalosporins were recommended; 2010-2012 to when multiple cephaloporins were recommended along with azithromycin co-treatment; and 2012-2019 to when only ceftriaxone 250mg along with azithromycin co-treatment was recommended.

The per-lineage analysis also addressed the question of what drove the growth of lineage 21, indicating that its expansion post-2010 was driven primarily by the presence of GyrA 91F/95A (Supplementary Figures and Tables Figure S33).

While the fitness contributions of the set of resistance determinants in our model accounted for much of the lineage dynamics, some dynamics remained unexplained. For each lineage, we computed the number of years in which the absolute value of the average of the sum of the residual and lineage background terms exceeded the threshold of 0.1, representing approximately 10% growth or decline in a given year. In 11/29 lineages (lineages 2-4, 11, 13, 15, 16, 23, 26-28), there was at least one such year, and in six of those (lineages 2-4, 11, 15, 27), there were at least 3 such years.

To investigate this pattern, we examined lineages 2, 3, and 4. Lineage 2 carried none of the determinants we included in our model and underwent substantial growth starting in 2012 and peaking in 2018. We revisited the resistance phenotypes and genotypes for this lineage and noted that the isolates in Lineage 2 carry *tetM*, which confers high-level resistance to tetracycline-class antibiotics [30]. We did not include *tetM* in our model because we lacked data on the extent of tetracycline-class antibiotics use for *N. gonorrhoeae* treatment and for syndromic treatment of known or presumed chlamydial co-infection and because none of the other lineages carry *tetM*. Lineages 3 and 4 had high residual effects for at least 3 years and carried none of the resistance determinants in our model. The large and consistently positive residual effects (Supplementary Figures and Tables Figure S15 and Supplementary Figures and Tables Figure S16) thus point to factors other than the antibiotic pressures examined here in shaping these two lineages' success.

DISCUSSION

Antibiotic exposure selects for resistant strains over their susceptible counterparts, whereas in the absence of antibiotics the resistant strains may suffer a fitness cost. While this relationship plays a central role in shaping microbial population dynamics, we have lacked quantitative estimates of the environmentally varying fitness effects of genetic elements in natural populations. Here, we used *N. gonorrhoeae* population genomics from large-scale surveillance data, detailed understanding of the genetics underlying antibiotic resistance, and data on antibiotic treatment to quantify the contribution of and the interactions among antibiotic resistance determinants and how these shaped *N. gonorrhoeae* AMR dynamics in the US over the study period (1993-2019).

Models of antibiotic use-resistance relationships typically treat all phenotypically resistant strains as if they have the same fitness costs and benefits [31]. However, our findings suggest that a single amino acid difference in a resistance determinant may result in markedly different dynamics. The fluoroquinolone resistance-conferring alleles of GyrA 91F/95G and 91F/95A have phenotypically similar levels of resistance in the context of ParC 86D/87R/91E; however, after fluoroquinolones were no longer recommended, GyrA 91F/95G was associated with a fitness cost whereas GyrA 91F/95A was associated with a benefit. In line with this, the rising prevalence of fluoroquinolone resistance in *N. gonorrhoeae*

(Supplementary Figures and Tables Figure S1) masked the replacement of lineages carrying GyrA 91F/95G with those carrying GyrA 91F/95A. To help distinguish whether this advantage was due to GyrA 91F/95A itself or a tightly linked variant, *in vitro* competition assays demonstrated that the GyrA 91F/95A-containing strain was more fit than an isogenic GyrA 91F/95G strain, supporting the hypothesis that single amino acid differences in resistance determinants can drive distinct evolutionary trajectories. Several potential explanations exist for this phenomenon. One possibility is that reduced fitness cost of GyrA 91F/95A facilitates an overall fitness benefit in the presence of bystander exposure to fluoroquinolones, whereas GyrA 91F/95G is simply too costly to provide a net benefit from bystander exposure to fluoroquinolone alone, in the absence of direct use. Another possibility is that there may be a fitness benefit irrespective of treatment exposure *in vivo*. Studies have characterized an *in vivo* advantage of *N. gonorrhoeae* fluoroquinolone-resistant *gyrA* mutants compared to those carrying wild-type GyrA 91S/95D in a mouse model [32] in the absence of fluoroquinolone administration. The marked difference in fitness between GyrA mutants is also consistent with *in vitro* estimates of fitness differences between resistant *gyrA* mutants in *E. coli*, as resistant *E. coli* GyrA 87G mutants were fitter than resistant 87Y mutants [8]. These results underscore the importance of accounting for pathways to resistance when analyzing and modeling antimicrobial resistance dynamics.

Lineages carrying GyrA 91F/95G lost fitness after fluoroquinolones were no longer recommended, and persistence of sublineages point to *N. gonorrhoeae*'s strategies for responding to this fitness change. In lineage 20, one sublineage reverted to the susceptibility-conferring GyrA 91S/95D allele. Others changed the *mtr* locus, and one acquired azithromycin resistance through the C2611T 23S rRNA mutation (Figure 2). At the same time, the sexual network in which the sublineages circulated appeared to change from men who have sex with men to heterosexuals (Supplementary Figures and Tables Figure S2). While the number of isolates and sublineages limited quantification of these phenomena, they suggest responses to pressures from both antibiotics and host environments.

Similarly, for mosaic *penA* 34, we saw clear evidence of a large growth rate advantage compared to the baseline type that does not carry any of the resistance determinants studied when the cephalosporin cefixime was recommended. This advantage was rapidly lost after the switch to ceftriaxone 250mg, consistent with the observed decline of cefixime resistance [33].

For PBP1 421P, we estimated a consistent small fitness defect across the study period (1993-2019).

PBP1 421P mainly provides penicillin resistance with only relatively modest increase in cephalosporin MICs [22], but the absence of a fitness benefit suggests this resistance phenotype was insufficient even in the context of cephalosporin use to confer an advantage. Moreover, the carriage of PBP1 421P in 12 of 29 lineages is consistent with at most a mild fitness defect. We conclude that it likely represents a relic of the era when penicillin was the backbone of *N. gonorrhoeae* infection treatment (Supplementary Figures and Tables Figure S1).

We estimated a large growth rate benefit of mosaic *mtrR* promoters once azithromycin co-treatment was introduced in 2010. This is consistent with the findings of continued rapid expansion of lineages carrying mosaic *mtrR* promoters noted in Europe [34], but we note that the interaction with other *mtrCDE* mosaics makes the overall picture challenging to interpret. In the dataset we used, mosaic *mtrR* promoters always co-occur with at least one of mosaic *mtrC* or *mtrD*, both of which have their own distinct fitness impacts (Supplementary Figures and Tables Table S2, Figure 6). The trajectory of the largest lineage carrying mosaic *mtrR* promoter, lineage 29, plateaus around 2015 (Supplementary Figures and Tables Figure S41). A similar behavior can be seen in the overall prevalence of azithromycin resistance (Supplementary Figures and Tables Figure S1), whereby the growth rate seems to decline post 2015. Possible explanations include a drop in azithromycin use [35] and sexual network-dependent fitness of the *mtrCDE* mosaics, as suggested by the over-representation of *mtrC* loss-of-function alleles in cervical specimens [36].

Investigating the fitness contributions at the level of individual lineages (Figure 7, Supplementary Figures and Tables Figures S13 to S40)) allowed us to interrogate how much of each lineage's growth trajectory can be explained by the combination of AMR and changes in treatment policy. This revealed an example of hitchhiking, where in Lineage 22 (Figure 7) the fitness cost incurred by one resistance determinant, GyrA 91F/95G, conferring resistance to fluoroquinolones, was outweighed by the fitness benefit from another resistance determinant, mosaic *penA* 34, conferring resistance to cephalosporins. Several lineages did not carry any of the determinants and displayed a consistent trend in their residual terms. In the case of Lineage 2 (Supplementary Figures and Tables Figure S14), we identified the presence of *tetM*, which confers resistance to tetracycline class antibiotics. This suggests that for some lineages, there may be a substantial impact of bystander exposure on their fitness trajectories [35, 37]. A similar phenomenon may explain the dynamics of Lineages 3 and 4. Incorporating population-wide antimicrobial use may enable quantification of the impact of bystander exposure. Lineages that

displayed large residual effects despite carrying resistance determinants included in our model may reflect the impact of lineage background, environment pressures, or bystander exposure, suggesting avenues for further investigation.

Our approach has limitations. First, we were only able to uncover sufficient signal in the data to quantify the impact of determinants that have a large effect or that appear on multiple lineage backgrounds. Even as we captured the dominant effects of resistance determinants, there was too much uncertainty to define the impact of many resistance determinants on fitness landscape of *N. gonorrhoeae*. Reducing the uncertainty requires either a larger number of sequences, more representative sampling, or both. This may also enable use of birth-death-sampling processes [38], especially variations of the multi-type birth-death process [39]. Larger sample sizes and higher data quality would enable more robust estimates under more complex models that could, for example, accommodate time-varying relationships between prescribing data and the growth rate effect of resistance determinants. Second, in our study, deviations from the model get captured by the residual terms. To include these phenomena, non-parametric methods such as splines or Gaussian processes could be used to model the relationship between treatment composition, time, and growth rate effect of determinants. Third, the need to explicitly define fixed lineages *a priori* is an approximation and may result in fragmentation of otherwise linked lineages. Fourth, the approach presented is only applicable for determinants that give rise to lineage-like dynamics. This effectively means that the estimates for the determinants are valid for sufficiently compatible genetic backgrounds where any putative fitness cost is not too large. If the fitness cost was large, the observed dynamics would likely resemble mutation-selection balance in the case of strong mutation and strong negative selection [7]. Fifth, our approach can only estimate the association between the presence of resistance determinants if carried by sufficiently successful or 'major' lineages. This effectively conditions on determinants being present on compatible genetic backgrounds, as it is unlikely that a clone would give rise to a major lineage in the absence of compatibility between the genetic background and the resistance determinant. Sixth, we have ignored any spatial heterogeneity in transmission and treatment. As the data collection is spatially very sparse, heterogeneity within the US in transmission and treatment is unlikely to impact the results. Lastly, importations from outside of the US may distort the results. Due to the focus on only major lineages, and the size of the *N. gonorrhoeae* epidemic in the US, we do not expect this to play a major role, and any remaining effects of importation should be compensated by the residual

over-dispersion terms in the statistical model.

Our results demonstrate how the expanding collection of microbial genomic data together with antibiotic prescribing data and phylodynamic modeling can be used to explain microbial ecological dynamics and quantify the fitness contributions of genetic elements in their changing *in vivo* environments. The power of this approach will be augmented with continued surveillance, sequencing, and systematic data collection, and the growing datasets will enable model refinement and development. While we focused on *N. gonorrhoeae* and AMR, these methods could be more broadly applied to other microbes and pressures, aiding in efforts to understand how combinations of genetic elements inform strain fitness across antimicrobial exposure, host niche, and other environmental pressures.

METHODS

Genomic Analysis

We collected publicly available genomic data, minimum inhibitory concentrations, and demographic data from GISP isolates (n = 5367) sequenced between years 2000 and 2019 [3, 13, 14, 15, 16]. *De novo* assembly was performed using SPAdes v 3.12.0 [40] with the –careful flag, and reference-based mapping to NCCP11945 (NC_011035.1) was done using BWA-MEM v 0.7.17 [41]. We used Pilon v 1.23 to call variants (minimum mapping quality: 20, minimum coverage: 10X) [42] after marking duplicate reads with Picard v 2.20.1 (https://broadinstitute.github.io/picard/) and sorting reads with samtools v 1.17 [43]. We generated pseudogenomes by incorporating variants supported by at least 90 % of reads and sites with ambiguous alleles into the reference genome sequence. We mapped reads to a single copy of the locus encoding the 23S rRNA and called variants using the same procedures [44].

We identified resistance-associated alleles from *de novo* assemblies and pseudogenomes. Likewise, we identified the presence of single nucleotide variants (e.g., mutations in *gyrA*, *parC*, *ponA*, and *penA*) and the copy number of resistance-associated variants in 23S rRNA from variant calls. To determine the presence or absence of genes, mosaic alleles, promoter variants, and small insertions or deletions we used the results of blastn v 2.9.0 [45] searches of assemblies for resistance-associated genes. We

typed mosaic *penA* alleles according to the nomenclature in the NG-STAR database [46]. We defined mosaic *mtr* alleles as those with <95% identity to the *mtr* operon encoded by FA1090 (NC_002946.2). Alleles were defined as loss-of-function (LOF) if frameshifts or nonsense mutations led to the translated peptide being less than 80% of the length of the translated reference allele.

Prior to phylogenetic reconstruction, we filtered assembled genomes based on the following criteria: (1) The total assembly length was longer than 1900000 bp and less than 2300000 bp. (2) Reference coverage was more than 30%. (3) Percentage of reads mapped to reference was at least 70%. (4) Less than 12% of positions were missing in pseudogenomes. This resulted in (n = 4573) retained samples.

A Lineage-Based Hierarchical Phylodynamic Model

Our aim was to study how interactions among six resistance-associated genes and operons–*gyrA*, *parC*, *ponA*, *penA*, the *mtr* operon, and the 23S rRNA–and the major antimicrobial classes used as primary treatment of gonorrhea between 1993-2019 (Supplementary Figures and Tables Table S1; [22, 47]) affected the success and failure of resistant *N. gonorrhoeae* lineages in the US. For *gyrA*, we considered alleles given by codons 91 and 95. For *ponA*, we considered the L and P variants encoded at codon 421. For *parC*, we considered alleles given by combinations of codons at positions 86, 87, and 91. For each of the loci that make up the *mtr* operon (*mtrC*, *mtrD*, *mtrR*, and the *mtr* promoter), we considered whether the locus was non-mosaic, mosaic, affected by a loss-of-function mutation, and whether there was an A-deletion in the *mtr* promoter. For *penA*, we considered variants at each site listed by NG-STAR *penA* allele types [46], along with whether the *penA* allele was mosaic. Within the lineages derived from our dataset, we only observed variation at codon sites 501 and 543 and the presence of the mosaic *penA* 34 allele. The mosaic *penA* 34 allele carries variants at other sites; however, since these variants do not occur on other backgrounds in the dataset, we could not estimate their contributions. The determinants at *parC* act as mutations modulating the impact of *gyrA* resistance mutations [25]. Consequently, we used partial pooling to estimate the effects of *gyrA* determinants across different *parC* contexts. For 23S rRNA we considered the presence of at least one copy carrying the C2611T substitution. While the 23S substitution A2059G is associated with a more dramatic increase in azithromycin resistance, we did not include it in any analysis as it appeared in fewer than 20 isolates.

We used phylodynamic modeling [48] to mitigate the impact of inconsistent sampling on reconstructing lineage ecology. Because phylodynamic modeling can be less sensitive than traditional incidence-based modeling to violations of sampling assumptions [49], it can accommodate the overrepresentation of antibiotic resistant specimens in collections of sequenced isolates[3, 13].

The data used in the statistical model consisted of (1) L genealogies $G = \{\boldsymbol{g}_i\}_{1 \leq i \leq L}$, each corresponding to a particular AMR-linked lineage (Figure 1); (2) resistance determinant presence by lineage (Table 1); and (3) treatment data from GISP clinics (Supplementary Figures and Tables Figure S1). As our aim was to quantify the impact of individual AMR determinants on lineage success and failure, we estimated the growth rate of the lineage-specific effective population size $r(t) = \dot{N}e(t)/Ne(t)$ [50, 24]. We extended prior work [50, 24] to a multiple lineage, multiple treatment, multiple AMR determinant scenario by constructing a hierarchical Bayesian regression model that accounted for intrinsic variation among lineages. We formulated the growth rate of the effective population size as a hierarchical linear model to estimate how much of lineage growth and decline could be explained as a function of the interaction between AMR determinants and the pattern of antimicrobial use. Disentangling the contributions of individual AMR determinants from external factors required accounting for the overall epidemic dynamics, for which we included a global trend term shared by all lineages; the effect of lineage background on baseline fitness, for which we included lineage-specific terms; and the over-dispersion in the growth and decline of individual lineages that occurs due to factors unaccounted for.

The growth rate of the effective population size serves as a proxy for lineage success and can be used to solve for the effective population size (Supplementary Methods Equation S2). While the effective population size is not necessarily directly proportional to incidence (it is a non-linear function of incidence and prevalence [49]), if fitness benefits are small in comparison to the per capita transmission rate $\beta(t)$ or if $\beta(t)$ is approximately constant, then the growth rate of the effective population size will approximately match the growth of the epidemic [50]. The effective population size can then be linked to individual genealogies via the coalescent likelihood (Supplementary Methods Equation S3). The key quantity of interest was the marginal impact of individual determinants on lineage growth rates. This is formulated in (Supplementary Methods Equation S5) and (Supplementary Methods Equation S6).

A detailed model characterization, including the regression equation, likelihood approximations, and

choice of priors, is in (Supplementary Methods A Hierarchical Phylodynamic Model).

Implementation

The model was implemented in the `stan` probabilistic programming language [51] and `R` language version 4.4.0 [52]. Sampling was performed using Hamiltonian Monte Carlo as implemented in `stan` [51]. Four chains were run in parallel for 1000 sampling iterations each. For all model parameters, the bulk effective sample size (bulk-ESS) was always at least 500, the $\hat{R}$ statistic always lower than 1.05 [53].

Lineage Assignment & Phylogenetic Reconstruction

We used `Gubbins` [54] to estimate recombining regions and `IQTree` [55] for phylogenetic reconstruction. The molecular clock model was $GTR{+}G{+}ASC$ as selected by `ModelFinder` [56].

We estimated the dates of ancestral nodes using the resulting tree with `BactDating` [57] under the additive relaxed clock model [58]. We estimated ancestral states for all determinants under study apart from the 23S rRNA as the joint maximum likelihood estimate under the F81 model [59] using `PastML` [60]. In the case of *penA*, the ancestral state reconstruction was performed using allele types and the resulting reconstruction was then mapped to *penA* determinants for subsequent analysis and lineage calling. For the 23S rRNA, we used maximum-parsimony ancestral reconstruction based on the DELTRAN algorithm [61] as implemented in `PastML` [60]. We chose this approach because the C2611T substitution is usually present in 4 copies, making reverse mutation unlikely, and DELTRAN prioritizes parallel mutation [61]. Furthermore, the 23S rRNA C2611T variant does not display a clonal pattern of inheritance (Supplementary Figures and Tables Figure S42).

We excluded samples with missing values in any of the determinants from the analysis prior to ancestral state reconstruction, leaving (n = 5215) samples. We defined a subset of tips as a lineage if it was the maximal subset such that there was no change of ancestral state in any of the loci across the unique path from each tip to the most recent common ancestor of the subset and the timing of the most recent common ancestor was estimated to no earlier than 1980 with at least 99% posterior probability. We

then defined included lineages in the analysis if they contained at least 30 tips.

GyrA Mutants Competition Assay

N. gonorrhoeae culture conditions

N. gonorrhoeae was cultured on GCB agar (Difco) supplemented with Kellogg's supplement (GCB-K) at 37°*C* with 5% CO2 [62]. We performed pairwise competition experiments in liquid GCP medium containing 15g/L proteose peptone 3 (Thermo Fisher), 1g/L soluble starch, 1g/L KH2PO4, 4g/L K2HPO4, and 5g/L NaCl (Sigma-Aldrich) with Kellogg's supplement [63].

Generation of isogenic *N. gonorrhoeae* strains and antibiotic susceptibility testing

Antibiotic susceptibility testing for ciprofloxacin was performed on GCB-K agar via Etest (BioMerieux). All minimum inhibitory concentration (MIC) results represent the mean of three independent experiments. Strains, plasmids and primers used in this study are listed in (Supplementary Figures and Tables Tables S4 to S6). All the isogenic *N. gonorrhoeae* strains were generated in a ciprofloxacin-resistant clinical isolate, GCGS0481, which carries GyrA 91F/95G and ParC 87R. To clone a GyrA 91S/95D fragment with a chloramphenicol resistant cassette (CMR), pAM_3 plasmid was constructed using Gibson assembly in a pUC19 [64] backbone. The GyrA 91S/95D fragment was amplified from pDRE77 [65] using the primer pair AM_7 and AM_8 and the chloramphenicol cassette from pKH37 [66] using the primer pair AM_9 and AM_10. Fragments were amplified using Phusion high-fidelity DNA polymerase (NEB), checked for appropriate size by gel electrophoresis, column purified (Qiagen PCR purification kit), assembled with Gibson Master Mix (NEB), and transformed into chemically competent DH5α *E. coli* (Invitrogen). Individual colonies were selected on LB agar supplemented with 20µg/mL chloramphenicol and grown overnight at 37°*C*. Plasmids were isolated using Miniprep Kit (Qiagen) according to the manufacturer's instructions and sequences were confirmed by Sanger sequencing. For the insertion of GyrA 91S/95D allele into *N. gonorrhoeae* GCGS0481, the isolate was grown overnight on a GCB-K plate at 37°*C* with 5% CO_2. After 16-20 hours, the strain was scraped and suspended in 0.3M sucrose (Sigma-Aldrich), electroporated with 200

ng of pAM_3 plasmid, and rescued with GCP medium supplemented with Kellogg's for 30 minutes. The transformants were then plated on non-selective GCB-K agar plates for 4-6 hours followed by selection on GCB-K plates supplemented with 4.5µg/mL chloramphenicol. Finally, individual colonies were re-streaked on non-selective GCB-K agar plates and the *gyrA* allele checked by Sanger sequencing. For cloning of GyrA 91F/95G and GyrA 91F/95A, fragments of *gyrA* were amplified using primers AM_5 (F) and AM_6 (R) from the genomic DNA of clinical *N. gonorrhoeae* isolates GCGS0481 and NY0842 respectively. Electroporation was done as described above, and individual colonies were selected on GCB-K plates supplemented with 2µg/mL ciprofloxacin. For all the transformations performed, transformations without DNA were used as negative controls.

Competitive fitness measurement of GyrA variants

GCGS0481 GyrA 91S/95D, GyrA 91F/95G and GyrA 91F/95A containing the CMR cassette were transformed with pDR53, a kanamycin cassette (KanR) derivative of pDR1 [67] (constructed using the primer pair DR_395 and DR_396). The resulting transformants were selected on GCB-K agar supplemented with 70µg/ml kanamycin. Colony PCR was performed to screen the kanamycin positive clones using the primer pair (DR_62 and DR_63) (Supplementary Figures and Tables Table S6). During the pairwise competition experiments, the competitive paired strains from overnight cultured plates (one kanamycin-sensitive and one kanamycin-resistant strain) were mixed and co-cultured (at a ratio of 1:1 by optical density) in antibiotic-free GCP media with Kellogg's supplement for 8 hours. At each timepoint, cultures were serially diluted, and same volume was plated on both GCB-K agar and GCB-K agar supplemented with 70µg/ml kanamycin. Finally, dilutions on both plates were quantified and the competitive index (CI) was calculated at each timepoint. The CI value at any timepoint was calculated as $(R_t/S_t)/(R_0/S_0)$ where R_t and S_t are the proportions of kanamycin-resistant and kanamycin-sensitive strains, respectively at any time point and R_0 and S_0 are the proportions of kanamycin-resistant and kanamycin-sensitive strains at time 0.

Code & Data Availability

The code and data necessary to reproduce the statistical analysis, along with the metadata and accession numbers for the isolates analyzed, are available at: `https://github.com/gradlab/GC_AMR_Lineages`.

AUTHOR CONTRIBUTIONS

DH and YHG conceptualized the study. DH and TDM designed and performed the computational analysis. AM designed and performed the competition assays. DH and YHG wrote the original draft. YHG acquired funding. DH, YHG, TDM, AM, SGP discussed the results and contributed to writing, reviewing, and editing of the manuscript.

ACKNOWLEDGMENTS

We thank Daniel H. F. Rubin for the pDR53 plasmid. This work was supported by NIH R01 AI132606 and R01 AI153521 to Y.H.G.

References

[1] Diarmaid Hughes and Dan I. Andersson. "Evolutionary Trajectories to Antibiotic Resistance". In: *Annual Review of Microbiology* 71.1 (Sept. 8, 2017), pp. 579–596. ISSN: 0066-4227, 1545-3251. DOI: 10.1146/annurev-micro-090816-093813. URL: https://www.annualreviews.org/doi/10.1146/annurev-micro-090816-093813 (visited on 06/18/2024).

[2] Paulo Durão, Roberto Balbontín, and Isabel Gordo. "Evolutionary Mechanisms Shaping the Maintenance of Antibiotic Resistance". In: *Trends in Microbiology* 26.8 (Aug. 1, 2018). Publisher: Elsevier, pp. 677–691. ISSN: 0966-842X, 1878-4380. DOI: 10.1016/j.tim.2018.01.005. URL:

https://www.cell.com/trends/microbiology/abstract/S0966-842X(18)30017-9 (visited on 06/18/2024).

[3] Yonatan H Grad et al. "Genomic epidemiology of gonococcal resistance to extended spectrum cephalosporins, macrolides, and fluoroquinolones in the US, 2000-2013". In: *J. Infect. Dis.* 214 (2016). ISBN: 7137456839, pp. 1579–1587. ISSN: 0022-1899. DOI: 10.1093/infdis/jiw420.

[4] François Blanquart et al. "The evolution of antibiotic resistance in a structured host population". In: *Journal of The Royal Society Interface* 15.143 (June 20, 2018), p. 20180040. DOI: 10.1098/rsif.2018.0040. URL: https://royalsocietypublishing.org/doi/full/10.1098/rsif.2018.0040 (visited on 04/17/2023).

[5] Hsiao-Han Chang et al. "Origin and proliferation of multiple-drug resistance in bacterial pathogens". In: *Microbiology and molecular biology reviews: MMBR* 79.1 (Mar. 2015), pp. 101–116. ISSN: 1098-5557. DOI: 10.1128/MMBR.00039-14.

[6] Sonja Lehtinen et al. "Evolution of antibiotic resistance is linked to any genetic mechanism affecting bacterial duration of carriage". In: *Proceedings of the National Academy of Sciences* 114.5 (Jan. 31, 2017), pp. 1075–1080. ISSN: 0027-8424, 1091-6490. DOI: 10.1073/pnas.1617849114. URL: https://pnas.org/doi/full/10.1073/pnas.1617849114 (visited on 06/17/2024).

[7] Pleuni S. Pennings. *Explaining the stable coexistence of drug-resistant and -susceptible pathogens: the Resistance Acquisition Purifying Selection model*. Pages: 2023.12.07.23299709. June 2, 2024. DOI: 10.1101/2023.12.07.23299709. URL: https://www.medrxiv.org/content/10.1101/2023.12.07.23299709v2 (visited on 07/01/2024).

[8] Sandra Trindade, Ana Sousa, and Isabel Gordo. "ANTIBIOTIC RESISTANCE AND STRESS IN THE LIGHT OF FISHER'S MODEL". In: *Evolution* 66.12 (Dec. 1, 2012), pp. 3815–3824. ISSN: 0014-3820. DOI: 10.1111/j.1558-5646.2012.01722.x. URL: https://doi.org/10.1111/j.1558-5646.2012.01722.x (visited on 09/18/2024).

[9] Aaron Hinz et al. "Unpredictability of the Fitness Effects of Antimicrobial Resistance Mutations Across Environments in Escherichia coli". In: *Molecular Biology and Evolution* 41.5 (May 1, 2024), msae086. ISSN: 1537-1719. DOI: 10.1093/molbev/msae086. URL: https://doi.org/10.1093/molbev/msae086 (visited on 09/11/2024).

[10] Christine Tedijanto et al. "Estimating the proportion of bystander selection for antibiotic resistance among potentially pathogenic bacterial flora". In: *Proceedings of the National Academy of Sciences* 115.51 (Dec. 18, 2018). Publisher: Proceedings of the National Academy of Sciences, E11988–E11995. DOI: 10.1073/pnas.1810840115. URL: https://www.pnas.org/doi/full/10.1073/pnas.1810840115 (visited on 08/07/2024).

[11] Thomas Belcher et al. "Immune responses to Neisseria gonorrhoeae and implications for vaccine development". In: *Frontiers in Immunology* 14 (2023), p. 1248613. ISSN: 1664-3224. DOI: 10.3389/fimmu.2023.1248613.

[12] *Global Progress Report on HIV, Viral Hepatitis and Sexually Transmitted Infections, 2021. Accountability for the Global Health Sector Strategies 2016-2021: Actions for Impact.* 1st ed. Geneva: World Health Organization, 2021. 1 p. ISBN: 978-92-4-002707-7.

[13] Jesse C. Thomas et al. "Evidence of Recent Genomic Evolution in Gonococcal Strains With Decreased Susceptibility to Cephalosporins or Azithromycin in the United States, 2014-2016". In: *The Journal of Infectious Diseases* 220.2 (June 19, 2019), pp. 294–305. ISSN: 1537-6613. DOI: 10.1093/infdis/jiz079.

[14] Kim M. Gernert et al. "Azithromycin susceptibility of Neisseria gonorrhoeae in the USA in 2017: a genomic analysis of surveillance data". In: *The Lancet. Microbe* 1.4 (Aug. 2020), e154–e164. ISSN: 2666-5247. DOI: 10.1016/S2666-5247(20)30059-8.

[15] Jennifer L. Reimche et al. "Genomic Analysis of the Predominant Strains and Antimicrobial Resistance Determinants Within 1479 Neisseria gonorrhoeae Isolates From the US Gonococcal Isolate Surveillance Project in 2018". In: *Sexually Transmitted Diseases* 48.8 (Aug. 1, 2021), S78–S87. ISSN: 1537-4521. DOI: 10.1097/OLQ.0000000000001471.

[16] Jennifer L. Reimche et al. "Genomic analysis of 1710 surveillance-based Neisseria gonorrhoeae isolates from the USA in 2019 identifies predominant strain types and chromosomal antimicrobial-resistance determinants". In: *Microbial Genomics* 9.5 (May 2023), mgen001006. ISSN: 2057-5858. DOI: 10.1099/mgen.0.001006.

[17] Centers for Disease Control and Prevention (CDC). "Update to CDC's Sexually transmitted diseases treatment guidelines, 2010: oral cephalosporins no longer a recommended treatment for gonococcal infections". In: *MMWR. Morbidity and mortality weekly report* 61.31 (Aug. 10, 2012), pp. 590–594. ISSN: 1545-861X.

[18] Kayla E. Hagman et al. "Resistance of Neisseria gonorrhoeae to antimicrobial hydrophobic agents is modulated by the mtrRCDE efflux system". In: *Microbiology* 141.3 (1995). Publisher: Microbiology Society, pp. 611–622. ISSN: 1465-2080. DOI: 10.1099/13500872-141-3-611. URL: https://www.microbiologyresearch.org/content/journal/micro/10.1099/13500872-141-3-611 (visited on 08/22/2024).

[19] Michael D. Karcher et al. "phylodyn: an R package for phylodynamic simulation and inference". In: *Molecular Ecology Resources* 17.1 (2017). _eprint: https://onlinelibrary.wiley.com/doi/pdf/10.1111/1755-0998.12630, pp. 96–100. ISSN: 1755-0998. DOI: 10.1111/1755-0998.12630. URL: https://onlinelibrary.wiley.com/doi/abs/10.1111/1755-0998.12630 (visited on 06/24/2020).

[20] J Maynard-Smith et al. "How clonal are bacteria?" In: *Proc Natl Acad Sci USA* 90.10 (May 1993), pp. 4384–8. ISSN: 0027-8424. URL: http://www.ncbi.nlm.nih.gov/pubmed/21513472.

[21] Leonor Sánchez-Busó et al. "The impact of antimicrobials on gonococcal evolution". In: *Nature Microbiology* 4.11 (Nov. 2019). Publisher: Nature Publishing Group, pp. 1941–1950. ISSN: 2058-5276. DOI: 10.1038/s41564-019-0501-y. URL: https://www.nature.com/articles/s41564-019-0501-y (visited on 06/03/2024).

[22] Walter Demczuk et al. "Equations To Predict Antimicrobial MICs in Neisseria gonorrhoeae Using Molecular Antimicrobial Resistance Determinants". In: *Antimicrobial Agents and Chemotherapy* 64.3 (Feb. 21, 2020), e02005. DOI: 10.1128/AAC.02005-19. URL: https://pmc.ncbi.nlm.nih.gov/articles/PMC7038236/ (visited on 11/21/2024).

[23] Koji Yahara et al. "Emergence and evolution of antimicrobial resistance genes and mutations in Neisseria gonorrhoeae". In: *Genome Medicine* 13.1 (Mar. 30, 2021), p. 51. ISSN: 1756-994X. DOI: 10.1186/s13073-021-00860-8. URL: https://doi.org/10.1186/s13073-021-00860-8 (visited on 01/08/2025).

[24] David Helekal et al. "Estimating the fitness cost and benefit of antimicrobial resistance from pathogen genomic data". In: *Journal of The Royal Society Interface* 20.203 (June 14, 2023). Publisher: Royal Society, p. 20230074. DOI: 10.1098/rsif.2023.0074. URL: https://royalsocietypublishing.org/doi/10.1098/rsif.2023.0074 (visited on 06/04/2024).

[25] Magnus Unemo and William M. Shafer. "Antibiotic resistance in Neisseria gonorrhoeae: origin, evolution, and lessons learned for the future". In: *Annals of the New York Academy of Sciences*

1230 (Aug. 2011), E19–E28. ISSN: 0077-8923. DOI: 10.1111/j.1749-6632.2011.06215.x. URL: https://www.ncbi.nlm.nih.gov/pmc/articles/PMC4510988/ (visited on 09/18/2024).

[26] Makoto Ohnishi et al. "Ceftriaxone-Resistant Neisseria gonorrhoeae, Japan". In: *Emerging Infectious Diseases* 17.1 (Jan. 2011), pp. 148–149. ISSN: 1080-6040. DOI: 10.3201/eid1701.100397. URL: https://www.ncbi.nlm.nih.gov/pmc/articles/PMC3204624/ (visited on 09/18/2024).

[27] Satoshi Ameyama et al. "Mosaic-Like Structure of Penicillin-Binding Protein 2 Gene (penA) in Clinical Isolates of Neisseria gonorrhoeae with Reduced Susceptibility to Cefixime". In: *Antimicrobial Agents and Chemotherapy* 46.12 (Dec. 2002), pp. 3744–3749. ISSN: 0066-4804. DOI: 10.1128/AAC.46.12.3744-3749.2002. URL: https://www.ncbi.nlm.nih.gov/pmc/articles/PMC132769/ (visited on 09/19/2024).

[28] Patricia A. Ropp et al. "Mutations in ponA, the gene encoding penicillin-binding protein 1, and a novel locus, penC, are required for high-level chromosomally mediated penicillin resistance in Neisseria gonorrhoeae". In: *Antimicrobial Agents and Chemotherapy* 46.3 (Mar. 2002), pp. 769–777. ISSN: 0066-4804. DOI: 10.1128/AAC.46.3.769-777.2002.

[29] Crista B. Wadsworth et al. "Azithromycin Resistance through Interspecific Acquisition of an Epistasis-Dependent Efflux Pump Component and Transcriptional Regulator in Neisseria gonorrhoeae". In: *mBio* 9.4 (Aug. 7, 2018), e01419–18. ISSN: 2150-7511. DOI: 10.1128/mBio.01419-18. URL: https://www.ncbi.nlm.nih.gov/pmc/articles/PMC6083905/ (visited on 01/30/2025).

[30] Tatum D. Mortimer and Yonatan H. Grad. "Applications of genomics to slow the spread of multidrug-resistant Neisseria gonorrhoeae". In: *Annals of the New York Academy of Sciences* 1435.1 (Jan. 2019), pp. 93–109. ISSN: 1749-6632. DOI: 10.1111/nyas.13871.

[31] François Blanquart. "Evolutionary epidemiology models to predict the dynamics of antibiotic resistance". In: *Evolutionary Applications* 12.3 (Mar. 2019), pp. 365–383. ISSN: 1752-4571, 1752-4571. DOI: 10.1111/eva.12753. URL: https://onlinelibrary.wiley.com/doi/10.1111/eva.12753 (visited on 06/17/2024).

[32] Anjali N. Kunz et al. "Impact of Fluoroquinolone Resistance Mutations on Gonococcal Fitness and In Vivo Selection for Compensatory Mutations". In: *The Journal of Infectious Diseases*

205.12 (June 15, 2012), pp. 1821–1829. ISSN: 0022-1899. DOI: 10.1093/infdis/jis277. URL: https://doi.org/10.1093/infdis/jis277 (visited on 07/30/2024).

[33] Lilith K. Whittles, Peter J. White, and Xavier Didelot. "Estimating the fitness cost and benefit of cefixime resistance in Neisseria gonorrhoeae to inform prescription policy: A modelling study". In: *PLOS Medicine* 14.10 (Oct. 31, 2017). Publisher: Public Library of Science, e1002416. ISSN: 1549-1676. DOI: 10.1371/journal.pmed.1002416. URL: https://journals.plos.org/plosmedicine/article?id=10.1371/journal.pmed.1002416 (visited on 06/18/2024).

[34] Daniel Golparian et al. "Antimicrobial-resistant Neisseria gonorrhoeae in Europe in 2020 compared with in 2013 and 2018: a retrospective genomic surveillance study". In: *The Lancet Microbe* 5.5 (May 1, 2024). Publisher: Elsevier, e478–e488. ISSN: 2666-5247. DOI: 10.1016/S2666-5247(23)00370-1. URL: https://www.thelancet.com/journals/lanmic/article/PIIS2666-5247(23)00370-1/fulltext (visited on 08/28/2024).

[35] Scott W Olesen et al. "Azithromycin Susceptibility Among Neisseria gonorrhoeae Isolates and Seasonal Macrolide Use". In: *The Journal of Infectious Diseases* 219.4 (Jan. 29, 2019), pp. 619–623. ISSN: 0022-1899. DOI: 10.1093/infdis/jiy551. URL: https://doi.org/10.1093/infdis/jiy551 (visited on 11/10/2024).

[36] Kevin C. Ma et al. "Adaptation to the cervical environment is associated with increased antibiotic susceptibility in Neisseria gonorrhoeae". In: *Nature Communications* 11.1 (Aug. 17, 2020). Publisher: Nature Publishing Group, p. 4126. ISSN: 2041-1723. DOI: 10.1038/s41467-020-17980-1. URL: https://www.nature.com/articles/s41467-020-17980-1 (visited on 10/28/2024).

[37] Scott W Olesen and Yonatan H Grad. "Deciphering the Impact of Bystander Selection for Antibiotic Resistance in Neisseria gonorrhoeae". In: *The Journal of Infectious Diseases* 221.7 (Apr. 1, 2020), pp. 1033–1035. ISSN: 0022-1899. DOI: 10.1093/infdis/jiz156. URL: https://www.ncbi.nlm.nih.gov/pmc/articles/PMC7360351/ (visited on 01/23/2025).

[38] Tanja Stadler. "Sampling-through-time in birth–death trees". In: *Journal of Theoretical Biology* 267.3 (Dec. 7, 2010), pp. 396–404. ISSN: 0022-5193. DOI: 10.1016/j.jtbi.2010.09.010. URL: https://www.sciencedirect.com/science/article/pii/S0022519310004765 (visited on 10/28/2024).

[39] Joëlle Barido-Sottani, Timothy G Vaughan, and Tanja Stadler. "A Multitype Birth–Death Model for Bayesian Inference of Lineage-Specific Birth and Death Rates". In: *Syst. Biol.* 69.5 (2020), pp. 973–986. ISSN: 1063-5157. DOI: 10.1093/sysbio/syaa016.

[40] Anton Bankevich et al. "SPAdes: A New Genome Assembly Algorithm and Its Applications to Single-Cell Sequencing". In: *Journal of Computational Biology* 19.5 (May 2012), pp. 455–477. ISSN: 1066-5277, 1557-8666. DOI: 10.1089/cmb.2012.0021. URL: http://online.liebertpub.com/doi/abs/10.1089/cmb.2012.0021 (visited on 02/18/2014).

[41] Heng Li. "Aligning sequence reads, clone sequences and assembly contigs with BWA-MEM". In: *arXiv:1303.3997 [q-bio]* (Mar. 2013). arXiv: 1303.3997. URL: http://arxiv.org/abs/1303.3997 (visited on 09/29/2015).

[42] Bruce J. Walker et al. "Pilon: An Integrated Tool for Comprehensive Microbial Variant Detection and Genome Assembly Improvement". In: *PLOS ONE* 9.11 (Nov. 2014), e112963. ISSN: 1932-6203. DOI: 10.1371/journal.pone.0112963. URL: http://journals.plos.org/plosone/article?id=10.1371/journal.pone.0112963 (visited on 03/24/2017).

[43] Heng Li et al. "The Sequence Alignment/Map format and SAMtools". eng. In: *Bioinformatics (Oxford, England)* 25.16 (Aug. 2009), pp. 2078–2079. ISSN: 1367-4811. DOI: 10.1093/bioinformatics/btp352.

[44] Steven R. Johnson et al. "Use of whole-genome sequencing data to analyze 23S rRNA-mediated azithromycin resistance". In: *International Journal of Antimicrobial Agents* 49.2 (Feb. 2017), pp. 252–254. ISSN: 0924-8579. DOI: 10.1016/j.ijantimicag.2016.10.023. URL: http://www.sciencedirect.com/science/article/pii/S0924857916303971.

[45] Christiam Camacho et al. "BLAST+: architecture and applications". eng. In: *BMC bioinformatics* 10 (2009), p. 421. ISSN: 1471-2105. DOI: 10.1186/1471-2105-10-421.

[46] W. Demczuk et al. "Neisseria gonorrhoeae Sequence Typing for Antimicrobial Resistance, a Novel Antimicrobial Resistance Multilocus Typing Scheme for Tracking Global Dissemination of N. gonorrhoeae Strains". In: *Journal of Clinical Microbiology* 55.5 (Apr. 25, 2017). Publisher: American Society for Microbiology, pp. 1454–1468. DOI: 10.1128/jcm.00100-17. URL: https://journals.asm.org/doi/10.1128/jcm.00100-17 (visited on 10/29/2024).

[47] David W. Eyre et al. "WGS to predict antibiotic MICs for Neisseria gonorrhoeae". In: *Journal of Antimicrobial Chemotherapy* 72.7 (July 1, 2017), pp. 1937–1947. ISSN: 0305-7453. DOI: 10.1093/jac/dkx067. URL: https://doi.org/10.1093/jac/dkx067 (visited on 11/21/2024).

[48] Bryan T. Grenfell et al. "Unifying the Epidemiological and Evolutionary Dynamics of Pathogens". In: *Science* 303.5656 (Jan. 16, 2004). Publisher: American Association for the Advancement of Science, pp. 327–332. DOI: 10.1126/science.1090727. URL: https://www.science.org/doi/10.1126/science.1090727 (visited on 05/10/2023).

[49] Erik M Volz and Simon D W Frost. "Sampling through time and phylodynamic inference with coalescent and birth – death models". In: *J. R. Soc. Interface* 11 (2014), p. 20140945.

[50] Erik M Volz and Xavier Didelot. "Modeling the Growth and Decline of Pathogen Effective Population Size Provides Insight into Epidemic Dynamics and Drivers of Antimicrobial Resistance". In: *Syst. Biol.* 67.4 (2018). Ed. by Jeffrey Townsend, pp. 719–728. ISSN: 1063-5157. DOI: 10.1093/sysbio/syy007. URL: https://academic.oup.com/sysbio/article/67/4/719/4844079.

[51] Bob Carpenter et al. "Stan: A probabilistic programming language". In: *J. Stat. Softw.* 76.1 (2017). ISSN: 15487660. DOI: 10.18637/jss.v076.i01.

[52] R Core Team. *R: A Language and Environment for Statistical Computing*. Vienna, Austria: R Foundation for Statistical Computing, 2021. URL: https://www.R-project.org/.

[53] Aki Vehtarh et al. "Rank-Normalization, Folding, and Localization: An Improved R hat for Assessing Convergence of MCMC". In: *Bayesian Anal.* 16.2 (2021). _eprint: arXiv:1903.08008v5, pp. 667–718. ISSN: 19316690. DOI: 10.1214/20-BA1221.

[54] Nicholas J. Croucher et al. "Rapid phylogenetic analysis of large samples of recombinant bacterial whole genome sequences using Gubbins". In: *Nucleic Acids Research* 43.3 (Feb. 18, 2015), e15–e15. ISSN: 0305-1048. DOI: 10.1093/nar/gku1196. URL: https://doi.org/10.1093/nar/gku1196 (visited on 05/21/2021).

[55] Bui Quang Minh et al. "IQ-TREE 2: New Models and Efficient Methods for Phylogenetic Inference in the Genomic Era". In: *Molecular Biology and Evolution* 37.5 (May 1, 2020), pp. 1530–1534. ISSN: 0737-4038. DOI: 10.1093/molbev/msaa015. URL: https://doi.org/10.1093/molbev/msaa015 (visited on 05/30/2023).

[56] Subha Kalyaanamoorthy et al. "ModelFinder: fast model selection for accurate phylogenetic estimates". In: *Nature Methods* 14.6 (June 2017). Publisher: Nature Publishing Group, pp. 587–589. ISSN: 1548-7105. DOI: 10.1038/nmeth.4285. URL: https://www.nature.com/articles/nmeth.4285 (visited on 08/26/2024).

[57] Xavier Didelot et al. "Bayesian inference of ancestral dates on bacterial phylogenetic trees". In: *Nucleic Acids Res.* 46.22 (Dec. 2018), e134–e134. ISSN: 0305-1048. DOI: 10.1093/nar/gky783. URL: https://academic.oup.com/nar/article/46/22/e134/5089898.

[58] Xavier Didelot, Igor Siveroni, and Erik M Volz. "Additive uncorrelated relaxed clock models for the dating of genomic epidemiology phylogenies". In: *Mol. Biol. Evol.* 38 (2021), pp. 307–317. ISSN: 0737-4038. DOI: 10.1093/molbev/msaa193. URL: https://doi.org/10.1093/molbev/msaa193.

[59] Joseph Felsenstein. "Evolutionary trees from DNA sequences: A maximum likelihood approach". In: *Journal of Molecular Evolution* 17.6 (Nov. 1, 1981), pp. 368–376. ISSN: 1432-1432. DOI: 10.1007/BF01734359. URL: https://doi.org/10.1007/BF01734359 (visited on 08/14/2024).

[60] Sohta A Ishikawa et al. "A Fast Likelihood Method to Reconstruct and Visualize Ancestral Scenarios". In: *Molecular Biology and Evolution* 36.9 (Sept. 1, 2019), pp. 2069–2085. ISSN: 0737-4038. DOI: 10.1093/molbev/msz131. URL: https://doi.org/10.1093/molbev/msz131 (visited on 08/14/2024).

[61] David L. Swofford and Wayne P. Maddison. "Reconstructing ancestral character states under Wagner parsimony". In: *Mathematical Biosciences* 87.2 (Dec. 1, 1987), pp. 199–229. ISSN: 0025-5564. DOI: 10.1016/0025-5564(87)90074-5. URL: https://www.sciencedirect.com/science/article/pii/0025556487900745 (visited on 11/21/2024).

[62] D. S. Kellogg et al. "NEISSERIA GONORRHOEAE. I. VIRULENCE GENETICALLY LINKED TO CLONAL VARIATION". In: *Journal of Bacteriology* 85.6 (June 1963), pp. 1274–1279. ISSN: 0021-9193. DOI: 10.1128/jb.85.6.1274-1279.1963.

[63] Joseph P. Dillard. "Genetic Manipulation of Neisseria gonorrhoeae". In: *Current Protocols in Microbiology* Chapter 4 (Nov. 2011), Unit4A.2. ISSN: 1934-8533. DOI: 10.1002/9780471729259.mc04a02s23.

[64] J. Norrander, T. Kempe, and J. Messing. "Construction of improved M13 vectors using oligodeoxynucleotide-directed mutagenesis". In: *Gene* 26.1 (Dec. 1983), pp. 101–106. ISSN: 0378-1119. DOI: 10.1016/0378-1119(83)90040-9.

[65] Daniel Hf Rubin, Tatum D. Mortimer, and Yonatan H. Grad. "Neisseria gonorrhoeae diagnostic escape from a gyrA-based test for ciprofloxacin susceptibility and the effect on zoliflodacin resistance: a bacterial genetics and experimental evolution study". In: *The Lancet. Microbe* 4.4 (Apr. 2023), e247–e254. ISSN: 2666-5247. DOI: 10.1016/S2666-5247(22)00356-1.

[66] Petra L. Kohler et al. "AtlA functions as a peptidoglycan lytic transglycosylase in the Neisseria gonorrhoeae type IV secretion system". In: *Journal of Bacteriology* 189.15 (Aug. 2007), pp. 5421–5428. ISSN: 0021-9193. DOI: 10.1128/JB.00531-07.

[67] Daniel H. F. Rubin et al. "CanB is a metabolic mediator of antibiotic resistance in Neisseria gonorrhoeae". In: *Nature Microbiology* 8.1 (Jan. 2023), pp. 28–39. ISSN: 2058-5276. DOI: 10.1038/s41564-022-01282-x.